Specific Cutting Force Coefficients Modeling of End Milling by Neural Network

Sin-Young Lee*
School of Mechanical Engineering, Kunsan National University
Jang Moo Lee
School of Mechanical and Aeronautical Engineering, Seoul National University

In a high precision vertical machining center, the estimation of cutting forces is important for many reasons such as prediction of chatter vibration, surface roughness and so on. The cutting forces are difficult to predict because they are very complex and time variant. In order to predict the cutting forces of end-milling processes for various cutting conditions, their mathematical model is important and the model is based on chip load, cutting geometry, and the relationship between cutting forces and chip loads. Specific cutting force coefficients of the model have been obtained as interpolation function types by averaging forces of cutting tests. In this paper the coefficients are obtained by neural network and the results of the conventional method and those of the proposed method are compared. The results show that the neural network method gives more correct values than the function type and that in the learning stage as the omitted number of experimental data increase the average errors increase as well.

Key Words : Specific Cutting Force Coefficients, End Milling, Cutting Dynamics, Chip Load, Neural Network, Cutting Experiments

1. Introduction

In milling processes, feedrates or depths of cut are often limited due to chatter which is undesirable vibration or deflections by cutting forces which are more than allowable (Boothroyd, 1981).

In a high precisision vertical machining center chatter vibration is easily generated by unbalanced masses of rotating parts or variations of cutting forces. In order to analyze the chatter characteristics of a machining center, it is necessary to identify the dynamic characteristics of the machine structure and cutting dynamics(Sridhar et al., 1968). Many researches have been proceed-

---
* Corresponding Author,
  E-mail : sinylee@ks.kunsan.ac.kr
  TEL : +82-654-469-4716 ; **FAX** : +82-654-469-4727
  School of Mechanical Engineering, Kunsan National University, 68, Miryong-dong, Kunsan, Chonbuk 573 -701, Korea. (Manuscript **Received** October 12, 1999; **Revised** January 7, 2000)

ed on dynamic characteristics of structures and many methods have been studied in order to predict the cutting forces of milling processes for various cutting conditions in the field of cutting dynamics. Constant circular cutting resistances and cutting forces ratio were used for the machining by helix end mills (Ber et al., 1988), and constant specific cutting pressures and cutting forces ratio were proposed in the cutting by straight end mills (Altintas and Ghan, 1992 and Minis et al., 1990). Specific cutting pressures for incremental tangential forces and the ratio of radial forces to tangential forces were expressed as exponential functions of average chip thickness per revolution (Tarng et al., 1995), and Kim et al. (1998) tried to analyze metal cutting by finite element analysis. Smith and Tlusty (1993) introduced a fixed cutting stiffness and considered the radial forces to be proportional to the tangential forces. A mathematical model was given based on chip loads, cutting geometries, and the relation between cutting forces and chip loads

(Kline et al., 1982). The specific cutting constants of this model were obtained from the average cutting forces obtaind from cutting experiments.

In this paper, in order to predict the cutting forces during end mill cutting in a machining center a mathematical model is used. The model is based on the instant chip loads, cutting geometries, and the relation between cutting forces and chip loads. To predict the cutting forces of end milling process with the model, cutting experiments were performed under various cutting conditions on a vertical machining center. The specific cutting force coefficients of the proposed model is obtained by using neural network (Rumelhart et al., 1986, Chong and Parlos, 1997, Shiotsuka et al., 1993, Demuth and Beale, 1993, and Asakawa et al., 1990) from the average cutting forces obtained from the cutting experiments. A program predicting the cutting forces under a given cutting condition was developed, and cutting forces was calculated under various cutting conditions and compared with experimental results.

2. Cutting Dynamics of Milling

The fundamental element of predicting cutting forces is chip loads which apply to a given cutting tool as shown in Fig. 1. The most familiar form among the equations proposed for chip thickness is Eq. (1).

$$t_c = f \sin\beta \qquad (1)$$

where t_c is the instantaneous chip thickness, f is the feed per flute and β indicates the angular position of the tool edge during cutting. The total chip load of an end mill for any instant is the sum of chip load of each thin disk divided along the axis of the cutting tool. Cutting force consists of the tangential cutting force component proportional to chip load and the radial cutting force component proportional to the tangential cutting force component (Kline et al., 1982).

$$\Delta F_{tan} = K_{To} D_z t_c \qquad (2)$$
$$\Delta F_{rad} = K_R \Delta F_{tan} \qquad (3)$$

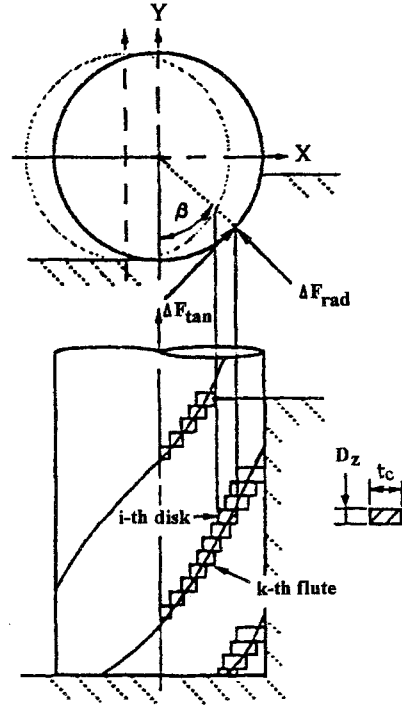where ΔF_{tan} is the tangential force component

Fig. 1 Concept of end-milling

for a small disk of the corresponding edge, ΔF_{rad} is the radial force component for the small disk, D_z is the width of a small disk divided in axial direction, t_c is the chip thickness shown in Eq. (1), K_{To} and K_R are constants obtained from experiments.

Specific cutting force coefficient K_{To} varies corresponding to the chip thickness, but it can be approximated as shown in Eq. (4) due to weak non-linearity (Kline et al., 1982).

$$\Delta F_{tan} = [C t_c^{-0.3}] D_z t_c = C D_z (f \sin\beta)^{0.7}$$
$$\approx K_T D_z f \sin\beta \qquad (4)$$

where C is a temporary proportional constant used to define specific cutting force coefficient.

The specific cutting force coefficient K_T of Eq. (4) varies according to various cutting conditions such as feed, depth of cut in radial and axial directions. Applying to a down milling case by the tool of radius Rad, number of flute N_f and the helix angle of a_{hx}, the angular position of a small disk in a flute can be expressed as follows:

$$\beta(i, k, t) = -\theta(t) + \frac{2\pi}{N_f}(k-1)$$

$$+ (i - \frac{1}{2}) D_z \cdot \frac{\tan \alpha_{hx}}{Rad} \qquad (5)$$

where i is the assigned number of a small disk in the axial direction, t is the lapse of time, and k is the assigned number of the corresponding flute. Some angular positions among $\beta(i, k, t)$'s contribute to cutting forces only when they are included in the cutting range. The tangential and radial cutting forces for small disks are dissolved into the global coordinates X, Y and the sums of the forces become the cutting forces in the global coordinates.

$$F_x(t) = \sum_{i=1}^{N_z} \sum_{k=1}^{N_f} \{-\varDelta F_{rad}(i, k, t) \sin\beta(i, k, t)$$
$$+ \varDelta F_{tan}(i, k, t) \cos\beta(i, k, t)\} \qquad (6a)$$

$$F_y(t) = \sum_{i=1}^{N_z} \sum_{k=1}^{N_f} \{\varDelta F_{rad}(i, k, t) \cos\beta(i, k, t)$$
$$+ \varDelta F_{tan}(i, k, t) \sin\beta(i, k, t)\} \qquad (6b)$$

(while $\beta(i, k, t)$ is in the cutting range)

Substituting Eqs. (3) and (4) into Eq. (6),

$$F_x(t) = K_T D_z f \sum_{i=1}^{N_z} \sum_{k=1}^{N_f} \{-K_R \sin^2\beta(i, k, t)$$
$$+ \sin\beta(i, k, t) \cos\beta(i, k, t)\} \qquad (7a)$$

$$F_y(t) = K_T D_z f \sum_{i=1}^{N_z} \sum_{k=1}^{N_f} \{K_R \sin\beta(i, k, t)$$
$$\cdot \cos\beta(i, k, t) + \sin^2\beta(i, k, t)\} \qquad (7b)$$

(while $\beta(i, k, t)$ is in the cutting range)

Therefore the cutting forces become functions of specific cutting force coefficients K_R and K_T and the cutting forces at any time can be estimated by obtaining the coefficients.

3. Determination of Specific Cutting Coefficients

3.1 Specific cutting force coefficients by least square method

If average cutting forces for a specific cutting condition (radial and axial depth of cut and feed for a given cutting tool) is obtained, K_R and K_T can be calculated from an experiment because average cutting forces are functions of specific cutting coefficients as shown in Eq. (7). K_R and K_T can be obtained for various cases where feed, radial and axial depths of cut change and expressed as the interpolation function of feed, radial

and axial depths of cut by the least square method (Kline et al., 1982) as in Eq. (8).

$$K_T = a_0 + a_1 RD + a_2 AD + a_3 f + a_4 RD$$
$$\cdot AD + a_5 f \cdot RD + a_6 f \cdot AD + a_7 RD^2$$
$$+ a_8 AD^2 + a_9 f^2 \qquad (8a)$$

$$K_R = b_0 + b_1 RD + b_2 AD + b_3 f + b_4 RD$$
$$\cdot AD + b_5 f \cdot RD + b_6 f \cdot AD + b_7 RD^2$$
$$+ b_8 AD^2 + b_9 f^2 \qquad (8b)$$

where RD is the radial depth of cut, AD is the axial depth of cut, f is the feed per flute, and $a_0 \sim a_9$ and $b_0 \sim b_9$ are coefficients for specific cutting force coefficients. The coefficients $a_0 \sim a_9$ and $b_0 \sim b_9$ in Eq. (8) are obtained from the cutting condition data and K_R and K_T corresponding to each cutting condition as shown in Eq. (9).

$$\begin{Bmatrix} a_0 \\ a_1 \\ a_2 \\ \vdots \\ a_9 \end{Bmatrix} = \begin{bmatrix} 1 & RD_1 & AD_1 & f_1 & \cdots & AD_1^2 & f_1^2 \\ 1 & RD_2 & AD_2 & f_2 & \cdots & AD_2^2 & f_2^2 \\ 1 & RD_3 & AD_3 & f_3 & \cdots & AD_3^2 & f_3^2 \\ \vdots & \vdots & \vdots & \vdots & \vdots & \vdots & \vdots \\ 1 & RD_n & AD_n & f_n & \cdots & AD_n^2 & f_n^2 \end{bmatrix}^+ \begin{Bmatrix} KT_1 \\ KT_2 \\ KT_3 \\ \vdots \\ KT_n \end{Bmatrix}$$
$$(9a)$$

$$\begin{Bmatrix} b_0 \\ b_1 \\ b_2 \\ \vdots \\ b_9 \end{Bmatrix} = \begin{bmatrix} 1 & RD_1 & AD_1 & f_1 & \cdots & AD_1^2 & f_1^2 \\ 1 & RD_2 & AD_2 & f_2 & \cdots & AD_2^2 & f_2^2 \\ 1 & RD_3 & AD_3 & f_3 & \cdots & AD_3^2 & f_3^2 \\ \vdots & \vdots & \vdots & \vdots & \vdots & \vdots & \vdots \\ 1 & RD_n & AD_n & f_n & \cdots & AD_n^2 & f_n^2 \end{bmatrix}^+ \begin{Bmatrix} KT_1 \\ KT_2 \\ KT_3 \\ \vdots \\ KT_n \end{Bmatrix}$$
$$(9b)$$

where $[\quad]^+$ means a pseudo-inverse matrix.

The above method is indicated as "Least square method A". Another method where the diameter of the cutting tool and the surface cutting speed (which are also parameters in cutting experiments) are added in order to improve the accuracy of modeling of the above method A and least square method is also used for obtaining the expressions for specific cutting coefficients is indicated as "Least square method B". Both methods are computer programmed.

3.2 Specific cutting force coefficients by neural network

A given cutting condition has various parameters such as tool diameter, radial and axial depths of cut, feed, and cutting speed. Accordingly, using three parameters as in Eq. (8) gives some error in

the result of cutting force calculation in cases where other parameters such as tool diameter, cutting speed and others are changed, although expressing specific cutting force coefficients K_R and K_T as function of feed, radial and axial depths of cut as in Eq. (8) by least square method are commonly used. Therefore in this paper a new modeling method using least square method is proposed, which includes tool diameter and cutting speed as input parameters. Also, a modeling method using neural network that obtains specific cutting force coefficients from many pairs of specific cutting force coefficients which is calculated from each given cutting conditions is tried. The input parameters in neural network are tool diameter, radial and axial depths of cut, feed, and cutting speed and the output parameters are specific cutting force coefficients in radial and tangential directions, K_T and K_R.

3.3 Neural network

Basic structure of neural network is composed of unit cells called neurons which have multiple inputs and single output (Rumelhart et al., 1986, Chong and Parlos, 1997, Shiotsuka et al., 1993, Demuth and Beale, 1993, and Asakawa et al., 1990). Internal state U_i^n and output O_i^n of each neuron is expressed using weighting coefficients $W_{j,i}^{n-1,n}$ and threshold θ_i^n. In this paper a modified sigmoid function was used as the output function $f(x)$ as shown in Eq. (10) instead of a standard sigmoid function type.

$$f(x) = \frac{2}{1 + \exp(-x/a)} - 1 \qquad (10)$$

where a is a constant showing a slope of each output function and its value is modified for various neurons in this paper. A 3-layer type neural network is used as shown in Fig. 2. Error back propagation method was used in learning the weighting coefficients and thresholds (Rumelhart et al., 1986). General modification method of weighting coefficients and thresholds between n-th layer and n-1 -th layer is Eq. (11).

$$W_{j,i}^{n-1,n}(t+1) = W_{j,i}^{n-1,n}(t) + \Delta W_{j,i}^{n-1,n}$$
$$\qquad (11a)$$

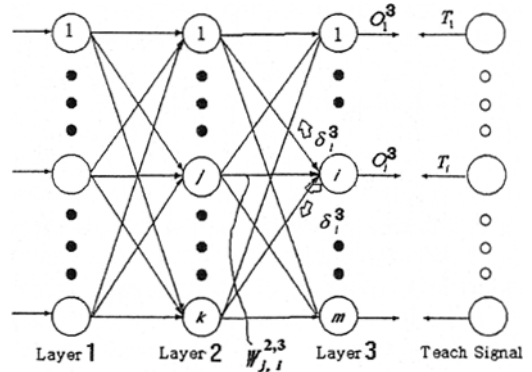$$\theta_i^n(t+1) = \theta_i^n(t) + \Delta\theta_i^n \qquad (11b)$$

Fig. 2 3 layer neural network

where, $\Delta W_{j,i}^{n-1,n} = -\varepsilon\dfrac{\partial J}{\partial W_{j,i}^{n-1,n}}$ and

$$\Delta\theta_i^n = -\varepsilon\frac{\partial J}{\partial\theta_i^n} \qquad (12)$$

J is the estimation function in the last output layer, ε is a positive constant and t represents the modification step number. Also the slope constants a's are modified similarly to Eq. (11).

$$a_i^n(t+1) = a_i^n(t) + \Delta a_i^n \ ; \ \Delta a_i^n = -\varepsilon\frac{\partial J}{\partial a_i^n}$$
$$\qquad (13)$$

Letting error signal in the last output layer, N-th layer (here $N=3$), as

$$\delta_i^N = \frac{\partial J}{\partial U_i^N} = -(T_i - O_i^N)f'(U_i^N) \qquad (14)$$

the modification volumes of weighting coefficients and thresholds between N-th layer and N − 1 -th layer becomes as follows:

$$\Delta W_{j,i}^{N-1,N} = -\varepsilon\delta_i^N O_j^{N-1}, \ \Delta\theta_i^N = -\varepsilon\delta_i^N \quad (15)$$

In this paper, 3-layer neural network is used because 2-layer was thought to be inadequate for describing some nonlinear system although it is simple and does not need much time in learning. As the number of layers in the neural network increases solving and learning the network system need much time.

The worst drawback of the error back-propagation method is that it may fall in a local minimum. In order to avoid this drawback, the following variations were added in identifying the characteristics of a system in this paper. At first, virtual impedance method (Asakawa et al., 1990)

as given in Eqs. (16) ~ (17) was used which considers the modification volumes two times before each step. Also, slopes of sigmoid output functions were also included as learning parameters and they were decided by the error back propagation method.

$$\Delta W_{j,i}^{n-1,n}(t) = -\varepsilon \delta_i^n O_j^{n-1} + \alpha_1 \Delta W_{j,i}^{n-1,n}(t-1)$$
$$+ \alpha_2 \Delta W_{j,i}^{n-1,n}(t-2) \qquad (16)$$

$$\Delta \theta_i^n(t) = -\varepsilon \delta_i^n + \alpha_1 \Delta \theta_i^n(t-1) + \alpha_2 \Delta \theta_i^n(t-2) \qquad (17)$$

$$\Delta a_i^n(t) = -\varepsilon \frac{\partial J}{\partial a_i^n} + \alpha_1 \Delta a_i^n(t-1)$$
$$+ \alpha_2 \Delta a_i^n(t-2) \qquad (18)$$

4. Cutting Experiments and Calculation of Specific Cutting Coefficients

4.1 Cutting experiments

Specific cutting force coefficients were experimentally determined by cutting experiments under various cutting conditions using a machining center. The constants in Eq. (8) were obtained by a program developed using the least square method. The machining center used in this study was TNV-40 manufactured by Tongil industries and the tool dynamometer used for measuring

cutting forces was 9257B manufactured by Kistler. The end mill was made of cemented carbide and had two flutes and 30° helix angle, −7° end cutting edge angle and 12° radial rake angle. The testpiece material was SM45C steel and its components were C (0.44%), Si (0.21%), Mn (0. 72%), P (0.02%), S (0.022%) and Fe (98.586%). Table 1 shows the cutting conditions used in the experiments, where feed was designated in the mm/min unit which is usually the input to a machining center. In calculations feed per flute was used by a simple conversion with number of flutes and revolutions per minute. Table 2 shows samples of average cutting forces obtained in the case of 16mm end mill diameter, and Table 3 shows samples in the case of 20mm end mill diameter. The experimental results showed that as

Table 1 Cutting conditions for tests

Diameters of cutter (mm)	16, 20
Radial depth of cut (mm)	2, 4, 6, 8, 10
Axial depth of cut (mm)	12, 20
Feedrate (mm/min)	67, 85, 120
Spindle speed (R. P. M.)	480, 600, 900

Table 2 Samples of average cutting forces for each cutting test (tool diameter 16mm)

No	Radial depth (mm)	Axial depth (mm)	RPM	Feed (mm/tooth)	Fx (N)	Fy (N)
1	2	20	600	0.07083	294.2	409.4
2	4	20	600	0.07083	457.5	763.7
4	8	20	600	0.07083	343.8	1523.
11	4	20	600	0.100	576.9	1035.
12	6	20	600	0.100	577.2	1584.
17	8	20	900	0.100	254.1	1369.
25	6	12	900	0.04722	141.7	557.9
26	8	12	900	0.04722	102.1	578.2
32	10	12	600	0.100	−127.4	1694.
36	8	12	900	0.06667	121.8	900.2
37	10	12	900	0.06667	−254.4	1154.

Table 3 Samples of average cutting forces for each cutting test (tool diameter 20 mm)

No	Radial depth (mm)	Axial depth (mm)	RPM	Feed (mm/tooth)	Fx (N)	Fy (N)
38	2	12	480	0.06979	171.6	199.3
39	4	12	480	0.06979	389.8	542.5
41	8	12	480	0.06979	190.3	1091.
48	4	12	480	0.08854	447.6	778.4
49	6	12	480	0.08854	480.5	1221.
56	2	20	480	0.06979	393.8	293.3
57	4	20	480	0.06979	557.4	884.4
62	6	20	600	0.05583	435.7	1328.
63	8	20	600	0.05583	353.4	1841.
73	8	20	600	0.07083	542.9	2998.
74	10	20	600	0.07083	231.0	3888.

Table 4 Coefficients of specific cutting forces in least square method A.

a_i	-0.831E10, -0.161E12, 0.810E12, 0.205E15, -0.450E12, 0.137E16, -0.121E16, 0.619E13, -0.207E14, -0.135E19
b_i	-0.443, 72.7, 46.98, 8590, -2987, -0.804E05, -0.153E06, -907, -577, -0.394E08

the radial depth of cut increases the force in the table feed direction increases but the force decreases after a specific value depending on the cutting condition although the resultant forces increase continuously. The results also showed that as the axial depth of cut increases the forces in three directions, namely in the table feed direction, the perpendicular direction, and the resultant force direction, increase. The resultant cutting forces are proportional to the sum of the cutting area. Table 4 shows the constants of specific cutting force coefficients calculated by the least square method, and Table 5 shows the comparisons between the specific cutting force coefficients obtained from cutting experiments and those obtained by the above constants. Table 6 shows the comparisons between the average cutting forces obtained from cutting experiments and those calculated by the constant of specific

cutting force coefficients given in Table 4.

4.2 Specific cutting force coefficients using neural network

The conventional method using the least square method like Table 4 makes relatively big errors as shown in Tables 5 and 6. Therfore, in this study the least square method which also includes tool diameter and cutting speed was used, and an approach which uses neural network for specific cutting force coefficients is proposed. A 3-layer network was used in the learning of neural network and five input parameters were used: tool diameter, radial depth of cut, axial depth of cut, feedrate, and cutting speed. The output parameters were specific cutting force coefficients of K_T and K_R. Initial values of weighting factors between the neurons in adjacent layers were set by small random numbers generated in the computer. Weighting factors, thresholds, and slopes of output functions were learned by varying the number of neurons in a hidden layer (the second layer). The variation of learning errors in cases of 25 and 30 neurons in the hidden layer is a thin curve as shown in Figs. 3 and 4 respectively, and thick curves in Figs. 3 and 4 show the average errors in each case respectively. Figure 5 shows the average

Table 5 Comparisons of specific cutting forces

Sample No	$K_T (\times 10^{10})$		K_R	
	Exper-iment	Calcula-ted	Exper-iment	Calcula-ted
1	0.4047	0.5324	0.5076	0.4589
2	0.3833	0.5211	0.3593	0.4566
11	0.3572	0.4110	0.3949	0.4387
12	0.3464	0.4194	0.3847	0.4245
25	0.3991	0.4139	0.5054	0.4536
26	0.3231	0.4067	0.4136	0.5064
32	0.3439	0.4337	0.5478	0.5219
36	0.3478	0.4849	0.4616	0.5116
37	0.3274	0.4945	0.7493	0.5563
38	0.4529	0.5233	0.4630	0.3782
39	0.6056	0.5011	0.3512	0.4230
48	0.6156	0.4681	0.4695	0.4284
49	0.6080	0.4624	0.4701	0.4654
57	0.5555	0.5214	0.4209	0.4567
62	0.5984	0.4957	0.5429	0.4574
63	0.6119	0.5018	0.5411	0.4600
73	0.7794	0.5314	0.5548	0.4505
74	0.8107	0.5529	0.5562	0.4468

Table 6 Comparisons of cutting forces

Sample No	$K_T (\times 10^{10})$		K_R	
	Exper-iment	Calcula-ted	Exper-iment	Calcula-ted
1	294.2	400.3	409.4	513.1
2	457.5	551.7	763.7	1124.
11	576.9	628.6	1035.	1234.
12	577.2	641.8	1584.	1968.
25	141.7	167.7	557.9	560.4
26	102.1	75.0	578.2	761.8
32	-127.4	-116.4	1694.	2116.
36	121.8	121.2	900.2	1286.
37	-254.4	-133.2	1154.	1629.
38	171.6	208.0	199.3	209.0
39	389.8	301.1	542.5	479.5
48	447.6	354.9	778.4	571.0
49	480.5	368.4	1221.	925.5
57	557.4	504.7	884.4	856.6
62	435.7	420.6	1328.	1037.
63	353.4	374.7	1841.	1440.
73	542.9	516.8	2998.	1924.
74	231.0	371.6	3888.	2515.

variation in learning errors versus number of neurons in the hidden layer. The 74 pairs of teach signals were used in Figs. 3~5. Table 7 shows the calculated specific cutting force coefficients and the average cutting forces using the result of learning in the case where the number of neurons in the hidden layer was 30. This case corresponds to case number 7 of NH30 in Table 8. The specific cutting force coefficients and the cutting forces are shown in Tables 5 and 6. Table 8 shows the average errors of the average cutting forces for the cases when the results of Table 4 (designated as LSM A) were, when tool diameter and cutting speed were added to the least square method (designated as LSM B), and when the neural network results where the number of hidden layer neurons were set as 30 or 35. Each neural network
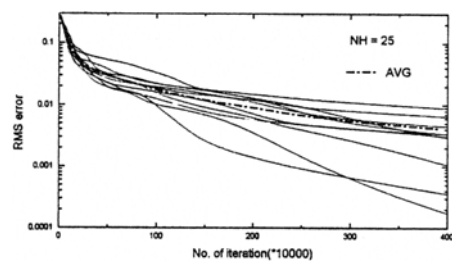
Fig. 3 Error trends when No. of neurons in hidden layer (NH) is 25

result shown in Table 8 is the result of total experimental data used in the learning of the neural network. It shows each result for 15 neural network cases learned independently and the average of each result. Tables 9 and 10 show the results of averages of errors for total experiments

Table 7 Calculation results using neural network

| Sample No	Specific cutting coefficient		Cutting forces (N)	
	$K_T \times 10^{10}$	K_R	Fx	Fy
1	0.4048	0.5076	294.3	409.2
2	0.3834	0.3594	457.5	763.9
11	0.3574	0.3949	577.2	1036.
12	0.3462	0.3847	576.9	1583.
25	0.3988	0.5057	141.4	557.5
26	0.3234	0.4137	102.1	578.8
32	0.3439	0.5479	-127.5	1694.
36	0.3476	0.4618	121.5	899.7
37	0.3274	0.7491	-254.2	1154.
38	0.4530	0.4631	171.6	199.4
39	0.6057	0.3512	389.9	542.5
48	0.6157	0.4695	447.6	778.5
49	0.6080	0.4702	480.4	1221.
57	0.5555	0.4209	557.5	884.5
62	0.5985	0.5430	435.6	1328.
63	0.6121	0.5410	353.7	1842.
73	0.7793	0.5549	542.5	2998.
74	0.8108	0.5562	231.1	3888.
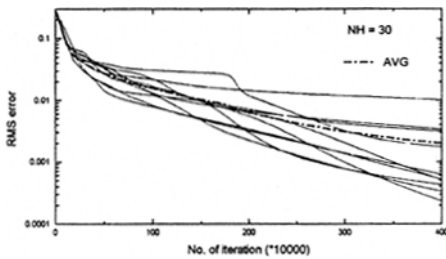
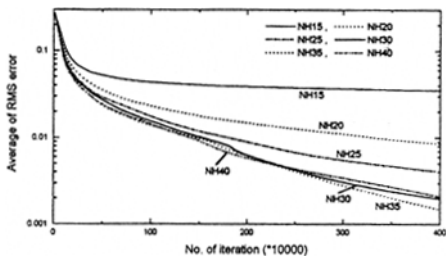**Fig. 4** Error trends when No. of neurons in hidden layer (NH) is 30

Fig. 5 Error trends with various No. of neurons in hidden layer

Table 8 Averages of errors by least square method (LSM) and neural networks.

Method	NH	Case	Errors (%) in average Fy	Errors (%) in average Fx
LSM A	–	–	33.1	31.3
LSM B	–	–	15.6	26.8
Neural Network	30	1	0.05	0.06
		2	0.03	0.04
		3	0.06	0.07
		4	0.03	0.05
		5	0.02	0.03
		6	0.31	0.33
		7	0.14	0.14
		8	0.08	0.09
		9	0.14	0.18
		⋮	⋮	⋮
		14	0.03	0.05
		15	0.09	0.13
		Avg.	0.15	0.19
	35	1	0.02	0.03
		2	0.04	0.05
		3	0.12	0.12
		4	0.18	0.03
		5	0.32	0.36
		6	0.15	0.19
		7	0.02	0.03
		8	0.08	0.10
		9	0.17	0.23
		⋮	⋮	⋮
		14	0.19	0.20
		15	0.02	0.04
		Avg.	0.11	0.13

after learning where some random data among the total experimental data were excluded in order to check the degree of prediction in cases where some of data were not learned. Table 9

**Table 9** Averages of errors by least square method (LSM) and neural networks for 68 set of experiments

Method	NH	Case	Errors (%) in average Fy	Errors (%) in average Fx
LSM A	–	–	33.7	31.4
LSM B	–	–	16.3	28.4
Neural Network	30	1	6.24	3.20
		2	7.08	23.7
		3	5.98	14.9
		4	6.25	19.5
		5	6.76	21.9
		6	5.53	3.74
		7	6.48	16.7
		8	8.75	5.57
		9	5.93	6.88
		⋮	⋮	⋮
		14	7.72	23.8
		15	7.06	21.3
		Avg.	6.58	15.5
	35	1	5.37	5.09
		2	5.57	7.77
		3	9.57	13.9
		4	5.15	7.93
		5	6.11	8.25
		6	7.60	25.5
		7	8.64	9.06
		8	6.92	4.17
		9	9.66	9.63
		⋮	⋮	⋮
		14	6.36	9.60
		15	7.41	15.2
		Avg.	6.96	11.4

Table 10 Averages of errors by least square method (LSM) and neural networks for 64 set of experiments

Method	NH	Case	Errors (%) in average Fy	Errors (%) in average Fx
LSM A	–	–	32.3	30.7
LSM B	–	–	15.4	27.5
Neural Network	30	1	9.45	17.1
		2	7.21	18.9
		3	13.7	12.8
		4	14.8	14.1
		5	9.77	21.6
		6	6.94	30.9
		7	4.23	22.7
		8	11.4	26.1
		9	9.60	14.9
		⋮	⋮	⋮
		14	15.2	14.4
		15	14.6	15.0
		Avg.	10.3	20.3
	35	1	5.63	19.5
		2	13.2	20.3
		3	14.2	19.3
		4	9.33	16.8
		5	15.8	23.5
		6	7.48	17.3
		7	12.0	11.1
		8	5.35	17.3
		9	5.25	21.5
		⋮	⋮	⋮
		14	13.1	16.4
		15	13.8	14.3
		Avg	11.3	17.9

shows the results in the case where random 6 experiments were excluded in learning, and Table 10 shows the results in the case where random 10 experiments were excluded. Figure 6 shows the averages of those shown in Tables 8~10.
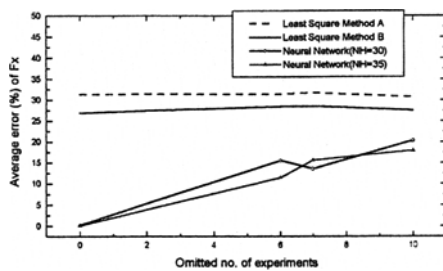
Figure 6 shows that the case where tool diameter and cutting velocity are added in obtaining specific cutting force coefficients using the least square method has smaller errors than the case where radial depth of cut, axial depth of cut, and
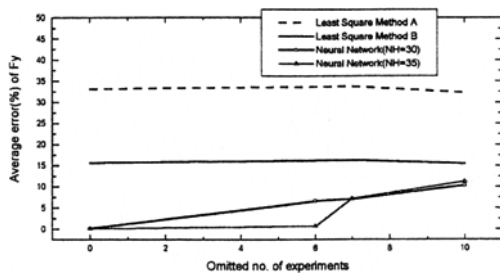
(a) Average error of y dircetional forces

(b) Average error of x dircetional forces

Fig. 6 Average errors with number of omitted experimental data

feed are used as input parameters. Also, the case where specific cutting force coefficients are obtained using neural networks has smaller errors than the above two cases. On the other hand F_y has smaller errors than F_x and this shows that there were more errors in the experimental measurement of F_x than F_y. Also as expected in Fig. 5, errors for the cases where the hidden layer has 30 neurons and the cases where the hidden layer has 35 neurons do not have remarkable differences. The results of investigation of the average errors for the cases where some of the experimental data were excluded in the learning of the neural network show that as the omitted number of experimental data increases the average errors increase.

5. Conclusions

In this paper, modelling for analysis and prediction of cutting forces in a machining center was discussed. The model was based on chip load, cutting geometry, and the relations between cutting forces and chip load. In order to predict the cutting forces of end milling processes with this model, cutting experiments were carried out under various cutting conditions.

The experimental results showed that as the radial depth of cut increases the force in the table feed direction increases but the force decreases after a specific value depending on the cutting condition although the resultant forces increase continuously. The results also showed that as the axial depth of cut increases the forces in three directions, namely in the table feed direction, the perpendicular direction, and the resultant force direction, increases. The resultant cutting forces are proportional to the sum of the cutting area.

The method for obtaining specific cutting force coefficients by the least square method using average cutting forces, radial and axial depths of cut, feed, tool diameter and cutting speed was proposed, and another method using neural network was proposed. Also the specific cutting force coefficients were calculated from total experimental data, as well as partial data with some data randomly excluded, and the results from three methods, namely, three and five input parameters least square methods, and neural network, were compared. The comparison showed that using the neural network resulted in relatively smaller error when the cutting forces of end mill processes were calculated. Also it showed that as the omitted number of experimental data increased the average errors increased.

References

Altintas, Y. and Ghan, Philip K., 1992, "In-Process Detection and Suppression of Chatter in Milling," *Int. J. Mach. Tool Des. Res.*, Vol. 32, No. 3, pp. 329~347.

Asakawa, K., Watanabe, N., Kawamura, A., Masuoka, R., Tanahashi, J., and Yamada, H., 1990, "Functions of Multi-Layered Neural Networks and their Fast Learning Algorithm," *Trans. of IEE (Japan)*, Vol. 110-C, No. 3, pp. 141~146.

Ber, A., Rotberg, J. and Zombach, S., 1988, "A Method for Cutting Force Evaluation of End Mills," *Annals of the CIRP*, Vol. 37/1, pp. 37 ~40.

Boothroyd, G., 1981, *Fundamentals of Metal Machining and Machine Tools*, McGraw-Hill International Book Co.

Chong, K. T. and Parlos, A. G., 1997, "Comparison of Traditional and Neural Network Approaches to Stochastic Nonlinear System Identification," *KSME International Journal*, Vol. 11, No. 3, pp. 267~278.

Demuth, H. and Beale, M., 1993, *Neural Network Toolbox User's Guide*, The MathWorks, Inc.

Kim, K. W., Lee, W. Y. and Sin, H. C., 1998, "Thermo-Viscoplastic Finite Element Analysis of Orthogonal Metal Cutting Considered Tool Edge Radius," *Trans. KSME*, Vol. 22(A), No. 1, pp. 1~15.

Kline, W. A., DeVor, R. E. and Lindberg, J. R., 1982, "The Prediction of Cutting Forces in End Milling with Application to Cornering Cuts," *Int. J. Mach. Tool Des. Res.*, Vol. 22, No. 11, pp. 7~22.

Minis, I., Yanushevsky, R. and Tembo, A., 1990, "Analysis of Linear and Nonlinear Chatter in Milling," *Annals of the CIRP*, Vol. 39/1, pp. 459~462.

Rumelhart, D. E., Hinton, G. E. and Williams, R. J., 1986, "Learning Representations by Back-propagating Errors," *Nature*, Vol. 323, pp. 533~536.

Shiotsuka, T., Ohta, K., Yoshida, K. and Nagamatus, A., 1993, "Identification and Control of Four-Wheel-Steering Car by Neural Network," *Trans. of JSME (Japan)*, Vol. 59(C), No. 559, pp. 708~713.

Smith, S. and Tlusty, J., 1993, "Efficient Simulation Programs for Chatter in Milling," *Annals of the CIRP*, Vol. 42/1, pp. 463~466.

Sridhar, R., Hohn, R. E. and Long, G. W., 1968, "A General Formulation of the Milling Process Equation," *Trans. ASME, Journal of Engineering for Industry*, Vol. 90, pp. 317~324.

Tarng, Y. S., Cheng, C. I. and Kao, J. Y., 1995, "Modeling of Three Dimensional Numerically Controlled End Milling Operations," *Int. J. Mach. Tool Des. Res.*, Vol. 35, No. 7, pp. 939~950.